INTL JOURNAL OF ELECTRONICS AND TELECOMMUNICATIONS, 2026, VOL. 72, NO. 1, PP. 1-6
Manuscript received September 10, 2025; revised January, 2026. doi: 10.24425/ijet.2026.157891

Single-frequency impedance monitoring of Li-ion 18650 cells for battery management applications

Krzysztof Kuliński

***Abstract*—This paper presents an impedance-based analysis of three types of cylindrical Li-ion 18650 cells subjected to controlled charge–discharge cycling under various temperatures and load conditions. The main objective was to evaluate whether single-frequency impedance monitoring can provide a reliable indicator of operational degradation that could be implemented in practical electronic systems. Measurements were performed using an RLC bridge in the frequency range of 42 Hz to 10 kHz, with particular emphasis on impedance at 100 Hz as a diagnostic reference point. Results demonstrate a clear correlation between impedance growth and the number of cycles, temperature, and discharge current, confirming the applicability of this method for real-time condition monitoring. The findings highlight the potential of simplified impedance diagnostics for integration into battery management systems (BMS), embedded electronics, and telecommunication power supply units, where compact, low-cost, and efficient diagnostic solutions are required.**

***Keywords*—Li-ion battery diagnostics; single-frequency EIS; battery management system (BMS); power electronics reliability**

I. Introduction

In recent years, the demand for reliable energy storage has rapidly increased, driven by the growth of embedded electronics, telecommunication systems, and power electronics applications. Lithium-ion (Li-ion) cells, particularly in the 18650 format, have become one of the most widely used solutions due to their high energy density and long cycle life. Ensuring durability and operational safety requires diagnostic methods that enable real-time monitoring of the technical condition of the cells [1,2].

One of the most effective electrochemical diagnostic methods is Electrochemical Impedance Spectroscopy (EIS), which enables the identification of processes occurring at the electrode–electrolyte interface, as well as the assessment of ion and electron transport parameters [1–3]. EIS measurements make it possible to determine, among other things, the series resistance (RS), charge transfer resistance (RCT), diffusion-related parameters (Warburg element), and capacitance changes associated with electrode degradation. Particular importance is placed on in-situ EIS measurements, conducted during actual cell operation – i.e., during charging or discharging. These measurements allow for the observation of dynamic changes in electrochemical parameters as a function of the state of charge (SoC) and state of health (SoH). Literature reports indicate that RCT) values are typically higher during discharge than during charge, which is attributed to the asymmetry of electrochemical processes and the presence of hysteresis [1,3]. Moreover, an increase in temperature and the number of charge-discharge cycles has been shown to intensify this effect [6,9,14].

Studies have shown that impedance characteristics are influenced not only by operational parameters (such as temperature, current, and depth of discharge) but also by the properties of electrode materials, including the size of active particles and the structure of the Solid Electrolyte Interphase (SEI) layer [2,4,6,12]. As degradation progresses, a systematic increase in both RCT and low-frequency impedance is observed, which can serve as an indicator of the cell's aging process [10,14].

In recent years, new measurement techniques have been developed, such as Dynamic Electrochemical Impedance Spectroscopy (DEIS) [3] and methods based on unipolar signal excitation [5], which enable galvanostatic measurements with high temporal resolution. These approaches allow for more precise analysis of cell behavior under real operating conditions while minimizing the influence of external disturbances and relaxation processes [7,13].

The aim of this study is to analyze impedance changes in three types of cylindrical Li-ion 18650 cells under different operating conditions, with particular attention to impedance at 100 Hz as a potential single-frequency diagnostic indicator. The results are discussed in the context of applicability in embedded electronic systems and BMS, where reliable and cost-effective monitoring of state of health (SoH) is essential.

II. Research Methodology

Three types of commercially available cylindrical lithium-ion 18650 cells were tested. The first was an LIR18650 (2600 mAh) from EEMB (cell no. 1) [15], the second a Li-ion EVE ICR18650-26V (2550 mAh, 7.65 A) (cell no. 2) [16], and the third a Samsung INR18650-35E (3500 mAh) (cell no. 3) [17]. These cells differ both in internal construction and in performance parameters declared by the manufacturers. Each cell was tested under varying ambient temperatures, discharge currents, and different stages of aging, defined by the number of full charge-discharge cycles. To ensure reproducibility and unambiguous interpretation of the results, a separate, factory-new cell was assigned for each combination of temperature (30°C, 40°C, 50°C) and discharge current (0.1C, 0.2C, 0.5C). This means that for each cell type, tests were performed on nine specimens, resulting in a total of 27 tested cells. During the tests,

This work was supported by the internal research grant for young researchers (SBM) of Faculty of Mining, Safety Engineering and Industrial Automation of Silesian University of Technology.

Author is with Silesian University of Technology, Poland (e-mail: krzysztof.kulinski@polsl.pl).

each battery underwent charge-discharge cycles conducted at constant currents corresponding to the assigned configuration, until reaching 300 cycles. Measurements were taken for new cells as well as after 100, 200, and 300 cycles.

An RLC bridge HIOKI 3532 was used to record impedance characteristics, enabling measurements in the frequency range from 42 Hz to 10 kHz. Due to the presence of the cell's electromotive force and potentially very low impedance values, a dedicated separation circuit was employed to eliminate the DC voltage component and protect the measurement path of the bridge. The schematic diagram of this circuit, based on publication [18], is shown in Figure 1. The circuit included coupling capacitors (10 µF in the current path and 3300 µF in the voltage path), loading resistors (100 kΩ), and an external voltage source controlling the charging process or allowing disconnection during discharging. The circuit was connected to the bridge in a four-wire configuration. Prior to each measurement series, a two-step calibration (for short and open circuit of the measurement path) was performed, enabling compensation for the influence of passive elements in the separation circuit on the final result.

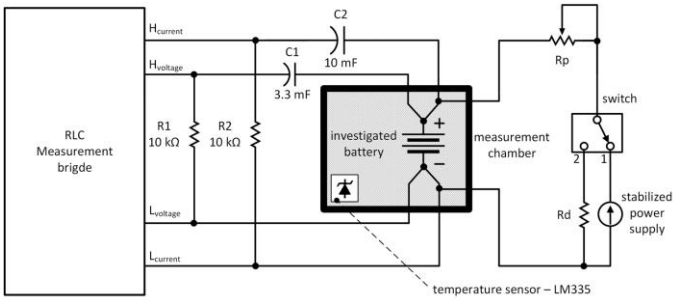

Fig. 1. Simplified model of the test stand including the climate chamber.

Measurements were carried out in situ, without interrupting the discharge process. Each measurement recorded the full impedance spectrum, including both impedance modulus and phase angle as functions of frequency. Due to the large number of combinations of test parameters - and thus the large number of resulting graphs - comparative analysis was carried out using extracted characteristic values. For each discharge cycle, the minimum and maximum values of the impedance modulus were defined as Z_{min} and Z_{max}, respectively. Similarly, the corresponding minimum and maximum impedance phase angles were extracted: $\angle Z_{min}$ and $\angle Z_{max}$, i.e. the extreme values recorded during the entire discharge cycle. In addition, the modulus and phase angle of the impedance at 100 Hz were highlighted as a reference. Due to the relatively stable behavior of the characteristics in this range, this parameter can serve as a practical diagnostic indicator of the cell's condition.

The collected data form the basis for further analysis of electrochemical parameters, such as actual resistance (R_{min}, R_{max}) and complex permittivity (X_{min}, X_{max}), which can be directly calculated from selected points on Nyquist or Bode plots. A total of 108 data sets were collected, covering all combinations of cell type, temperature, discharge current and number of cycles. This structured data set enables a comprehensive analysis of the impact of operating conditions on the cell's condition, stability and rate of electrochemical degradation.

III. Results

This section presents the results of impedance analysis of three types of 18650 lithium-ion cells, tested for the effect of operating conditions on their electrochemical parameters. The analysis focused on changes in the impedance modulus and phase angle only at a frequency of 100 Hz, chosen as a representative diagnostic point. This frequency was chosen because of the stability of the characteristics in this range and its sensitivity to changes associated with chemical and structural degradation of the cell.

For each combination of temperature, discharge current and number of cycles, minimum and maximum values of impedance modulus ($|Z_{min}|$ and $|Z_{max}|$) and phase angle ($\angle Z_{min}$ and $\angle Z_{max}$) were determined during the cell's discharge process, all measured at a constant frequency of 100 Hz. This approach reduced data redundancy while maintaining the high diagnostic value of the results.

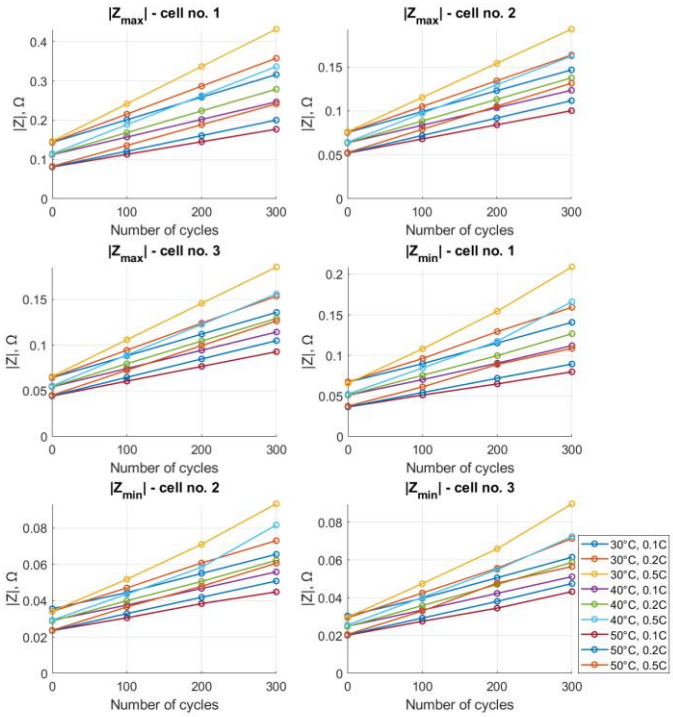

Fig. 2. Impedance modulus |Z| as a function of the number of cycles at 100 Hz, showing the maximum and minimum values recorded during discharge for each cell type for each case.

Fig. 2 shows the changes in maximum and minimum impedance modulus at 100 Hz for the three cell types analyzed, each tested separately. For each cell, a systematic increase in both $|Z_{max}|$ and $|Z_{min}|$ is observed as the number of cycles increases. This clearly indicates progressive electrochemical degradation, manifested by an increase in SEI layer resistance and reduced ionic transport.

Cell no. 1 (EEMB) shows the highest impedance values, especially under conditions of increased temperature and higher discharge current (e.g., 50°C, 0.5C). In contrast, no. 2 (EVE) and no. 3 (Samsung) cells show lower impedance values, which may suggest more favorable material properties or better structural stability. The increasing difference between $|Z_{max}|$ and $|Z_{min}|$ as the number of cycles increases (i.e., ΔZ increases) may

further indicate increasing nonlinear effects or a decrease in the intrinsic uniformity of the cell's impedance response.

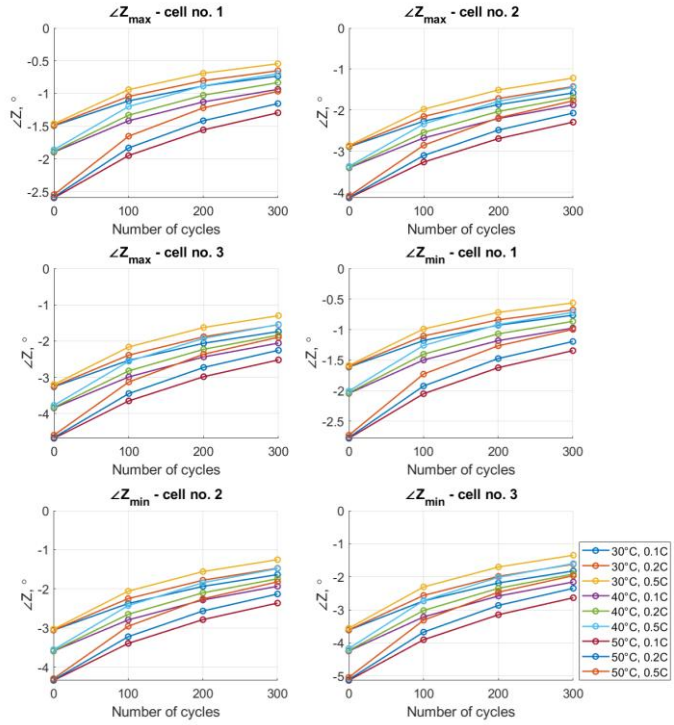

Fig. 3. Phase angle ∠Z as a function of the number of cycles at 100 Hz, showing the maximum and minimum values recorded during discharge for each cell type for each case.

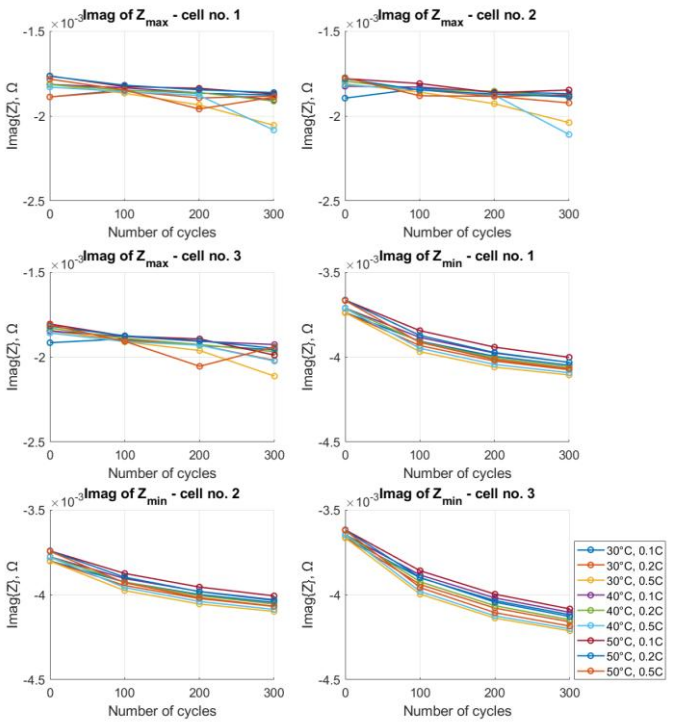

Fig. 4. Imaginary part of impedance Imag{Z} as a function of the number of cycles at 100 Hz, showing the maximum and minimum values recorded during discharge for each cell type for each case.

In the case of Imag{Z_{max}} the changes are less obvious - the values remain relatively stable with a slight downward trend accompanied by slight fluctuations, especially for cells 1 and 3 at higher currents and temperatures. This may indicate that this characteristic is more sensitive to transient changes in charge state or diffusion-related effects. The most pronounced systematic decrease in Imag{Z_{min}} occurs in cells 2 and 3, suggesting their greater susceptibility to capacity loss during operation. It is worth noting that the range of changes in Imag{Z} is on the order of several milliohms, confirming the need for precise measurement setup and careful interpretation of the results.

Fig. 5 shows the variation of the real part of the impedance (Real{Z}) as a function of the number of charge/discharge cycles for three types of lithium-ion cells, measured at a constant frequency of 100 Hz. The minimum and maximum values of Real{Z}, labeled Real{Z_{min}} and Real{Z_{max}}, were determined for each discharge cycle. Since the imaginary part of the impedance in this frequency range is orders of magnitude smaller than the real part (Imag{Z} ≪ Real{Z}), the real part of Z is almost identical to the impedance modulus. Therefore, the Real{Z} trends closely match the |Z| trends shown in fig. 2.

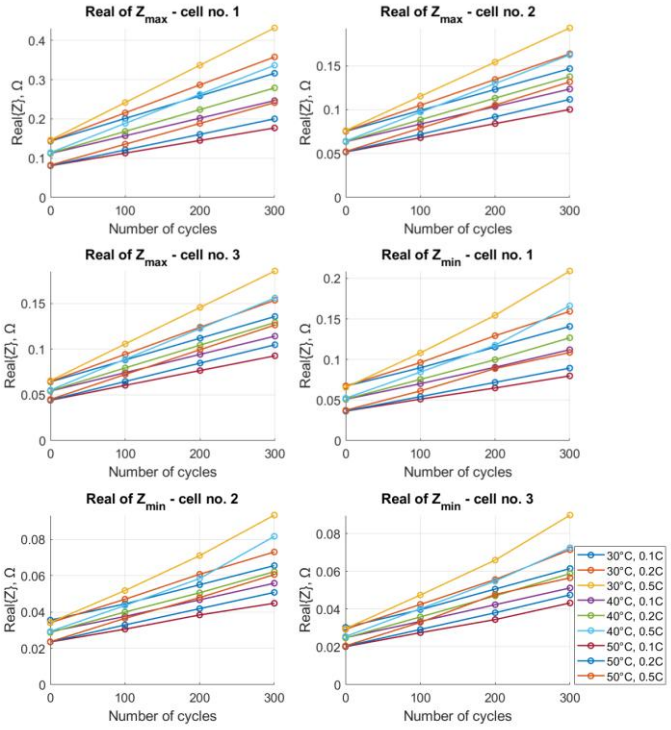

Fig. 5. Real part of impedance Real{Z} as a function of the number of cycles at 100 Hz, showing the maximum and minimum values recorded during discharge for each cell type for each case.

The second set of graphs (fig. 3) shows changes in the maximum and minimum values of the impedance phase angle (∠Z) at the same frequency of 100 Hz. Again, a clear trend can be observed: the phase angle increases (its absolute value decreases), indicating that the electrochemical response of the cell is shifting towards a more resistive behavior. Cell no. 2 (EVE) exhibits the most negative initial phase angle values (approximately –4°), but also shows the most pronounced reduction in absolute phase angle over the course of cycling. This may indicate a high degree of dynamic changes in the SEI

structure or a significant influence of current and temperature on capacitive and diffusive mechanisms. As with impedance magnitude, elevated temperatures and discharge currents clearly have a detrimental effect, accelerating changes in phase-related parameters.

Fig. 4 shows changes in the imaginary part of the impedance, Imag{Z}, for three types of lithium-ion cells at 100 Hz as a function of the number of discharge cycles. Both the minimum and maximum values of Imag{Z} recorded during each discharge cycle are shown. The Imag{Z} values are negative, indicating a capacity-dominated behavior of the cell's response at this frequency. For all cells, a gradual decrease in Imag{Z_{min}} is observed as the number of cycles increases, which may reflect a deterioration in the charge storage capacity at the electrode-electrolyte interface (e.g., a reduction in double-layer capacitance or modifications to the SEI layer).

An analogous and clear increase in Real{Z} with the number of cycles is observed, confirming the ongoing degradation processes affecting both electronic and ionic conductivity within the cell structure. The difference between Real{Z_{min}} and Real{Z_{max}} also grows over time, which can be interpreted as a manifestation of deteriorating structural homogeneity or an increased impact of localized transport limitations in the electrode material. The conclusions drawn from the changes in Real{Z} align with the analysis of |Z| and reinforce the proposition that the real part of impedance can serve as a diagnostic indicator of the cell's state of health under real operating conditions.

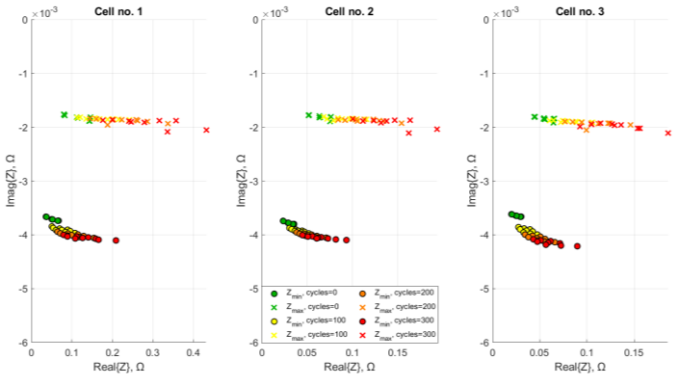

Fig. 6. Projection of complex impedance Z = Real{Z} + j·Imag{Z} at 100 Hz, showing the maximum and minimum values recorded during discharge for each cell type for each case (Nyquist-like plot).

Fig. 6 shows the distribution of data points representing the real (Real{Z}) and imaginary (Imag{Z}) components of impedance for the three lithium-ion cells tested, shown in two variants: corresponding to Z_{min} (marked with circles) and Z_{max} (marked with crosses). All measurements were made at a constant frequency of 100 Hz.

The points associated with Z_{max} form an almost horizontal line, which is consistent with the previously observed almost constant values of Imag{Z_{max}}. At the same time, the values of Real{Z_{max}} systematically increase with the number of cycles, reflecting the progressive increase in the cell's internal resistance. For the Z_{min} points, a slight curvature of the graph is observed, indicating a certain degree of variation of Imag{Z_{min}} depending on the number of cycles and operating conditions. This characteristic clearly shifts to the right, toward higher values of Real{Z}, which can be interpreted as a consequence of degradation of the electrode material and increasing charge transport resistance. Although this type of projection is based on a single frequency, it provides a convenient way to visualize changes in the state of the cells and allows tracking their position in "impedance space" during operation.

The analysis showed that the impedance of lithium-ion cells undergoes systematic changes during operation, which can be clearly correlated with an increase in the number of charge and discharge cycles. Both the minimum and maximum values of the impedance modulus increase as the cell ages, with the fastest increase observed under conditions of increased temperature (50°C) and higher discharge current (0.5C). This increase in |Z| can be interpreted as the result of thickening of the SEI layer, microcracks in the electrode material structure or changes in the electrolyte composition.

In parallel with the increase in the impedance modulus, a gradual decrease in the absolute value of the phase angle ∠Z was observed, indicating a loss of capacitive properties in the electrochemical system. This is typical of the progressive degradation of the double layer and weakening of the intercalation reaction. The imaginary part of the impedance (Imag{Z}) changed more slowly, maintaining small negative values - suggesting that the resistive component remains dominant at the 100 Hz frequency point. Analysis of Real{Z} confirmed that the impedance modulus at 100 Hz can serve as a good approximation of the actual resistance, since the imaginary part is usually two orders of magnitude smaller. Therefore, the measurement of |Z| at a single frequency can be used as a quick method to assess the health of a cell.

Additional insight was provided by an analysis of the scatter of complex impedance points in the plane of Real{Z} - Imag{Z}, where a characteristic shift of the points to the right was observed as the number of cycles increased (i.e., the resistance increased). The Z_{max} points formed an almost horizontal line, while the Z_{min} points followed a slightly curved trajectory, which may reflect differences in the cell's behavior depending on the specific operating point in the discharge cycle.

The results confirm the usefulness of impedance measurements at a single selected frequency (here: 100 Hz) as a diagnostic tool for assessing the cell's aging and comparing its characteristics under different thermal and current conditions. In future research, it would be worthwhile to extend this method in the direction of modeling changes in impedance parameters with simple indicators that could be implemented in real-time (on-line) in battery management systems (BMS).

IV. Discussion

The impedance measurements obtained for lithium-ion cells at a frequency of 100 Hz confirm previous literature findings regarding the influence of operating conditions on the electrochemical parameters of batteries [1, 3, 6, 14]. Both the impedance modulus and its real and phase components show a clear dependence on the number of charge/discharge cycles, ambient temperature, and current level. This indicates that impedance measured even at a single, fixed frequency can serve as a useful indicator of the technical condition of a cell.

Observations suggest that the most significant factor affecting the increase in impedance is the number of cycles, which is consistent with in-situ studies reported in [1] and [2],

among others. The increase in impedance can be attributed to the progressive degradation of the electrode structure, an increase in the resistance of the SEI layer, reduced ion mobility and micro-damage in the active material. The gradual decrease in phase angle (∠Z) over time simultaneously indicates a weakening of capacitive effects - potentially due to loss of active surface integrity or changes in electrode porosity and morphology.

The nearly linear relationship observed between the actual resistance Real{Z} and the number of cycles under specific conditions of temperature and discharge current, along with its strong correlation with |Z| at 100 Hz, suggests the potential of a simplified diagnostic model. Instead of analyzing the full impedance spectrum, such a model could be based on selected measurement points (e.g., |Z| and ∠Z at 100 Hz), significantly reducing cost and hardware requirements for practical applications.

From a practical point of view, these findings are valuable for battery management systems (BMS), especially in applications with stable or repeatable operating conditions (e.g., industrial equipment, emergency power systems). Continuous impedance monitoring at a constant frequency can provide a basis for predictive assessment of a cell's state of health (SoH) and even estimation of remaining useful life (RUL).

While Electrochemical Impedance Spectroscopy (EIS) provides the most comprehensive view of cell behavior, its implementation in practical electronic systems remains challenging due to hardware and time requirements. In contrast, the single-frequency method evaluated in this work offers a simplified yet sufficiently accurate diagnostic tool. Table I compares the two approaches, highlighting the trade-off between diagnostic detail and practical applicability.

TABLE I
COMPARISON OF FULL-SPECTRUM EIS AND SINGLE-FREQUENCY APPROACH

Feature	Full-spectrum EIS	Single-frequency (e.g. 100 Hz)
Hardware complexity	High (potentiostat, FRA)	Low (μC + simple circuitry)
Measurement time	Long (minutes)	Short (seconds)
Information content	Detailed electrochemical model	Simplified diagnostic indicators
Cost	High	Low
Suitability for BMS	Limited	High
Suitability for telecom/IoT	Low	High

As shown in Table I, the proposed single-frequency measurement at 100 Hz significantly reduces hardware complexity and measurement time, while still providing robust indicators of cell degradation. This makes it well suited for integration into microcontroller-based diagnostic modules, BMS architectures, and telecommunication power systems, where cost, reliability, and compactness are critical.

It should be noted, however, that limiting the analysis to a single frequency carries some limitations - measurements at 100 Hz do not allow resolution of all elements in the equivalent circuit, such as diffusion components (Warburg elements) or distributed time constants (CPE - Constant Phase Elements), which dominate at lower frequencies [10, 12]. Nevertheless, in many engineering applications, this simplified approach may be sufficient, especially where detection of general trends is more important than precise analysis of the physicochemical mechanism.

Additionally, the variability of ∠Z and Imag{Z} for Z_{min} can potentially serve as an indicator of changes in the discharge process dynamics – as suggested by the slight curvature observed in the complex plane trajectories. This opens up the possibility for new methods of classifying cell condition not only based on impedance magnitude but also on its intra-cycle variability.

A comparison with previous studies confirms both consistency and novelty of the obtained results. Literature reports often indicate that impedance growth with cycling is strongly related to SEI thickening, electrode cracking, and electrolyte decomposition [1, 6, 12]. However, most of these studies focus on full EIS spectra and use laboratory-grade potentiostats, which limits their transferability to engineering practice. In contrast, the present work demonstrates that single-frequency monitoring, restricted to 100 Hz, is sufficient to capture the same degradation trends. This simplification is in line with recent findings presented in [5, 7, 13], but the scope of this study – covering three cell types, three temperature levels, and three current conditions – provides a broader validation framework compared to earlier works, which usually investigate a single cell chemistry or a narrow operational range.

From a practical perspective, the results are highly relevant to electronic applications, particularly battery management systems (BMS) used in embedded devices, telecommunication power supplies, and backup units. Continuous monitoring at a fixed frequency can be implemented with compact hardware consisting of a microcontroller, a signal generator, and a simple measurement circuit, avoiding the need for costly frequency-response analyzers. For telecommunication infrastructure, where batteries are often deployed in remote or unattended locations, such an approach offers significant benefits: low maintenance cost, early detection of degradation, and the possibility of predictive replacement scheduling.

Moreover, the ability to characterize cells with minimal hardware resources makes the method suitable for Internet-of-Things (IoT) platforms, where compactness and energy efficiency are critical. Single-frequency impedance measurements could be periodically performed during idle states of the device, allowing condition monitoring without disturbing normal operation. The proposed diagnostic approach therefore bridges the gap between advanced electrochemical characterization and practical electronic implementation, supporting the development of next-generation BMS architectures.

V. Conclusions

This study confirmed that the impedance of lithium-ion 18650 cells undergoes systematic changes during cycling, with strong correlations to temperature, discharge current, and the number of charge–discharge cycles. A clear increase in impedance was observed under elevated stress conditions, demonstrating that degradation can be reliably tracked using simplified impedance analysis.

The results show that impedance at a single frequency (100 Hz) provides a robust approximation of cell resistance and correlates well with overall degradation trends. This makes it a practical diagnostic parameter that can be measured with relatively simple electronic circuitry, without the need for full-spectrum impedance spectroscopy.

From the perspective of electronic and telecommunication applications, the findings highlight the potential of implementing low-cost, single-frequency impedance monitoring in battery management systems (BMS), backup power units, and embedded monitoring platforms. Such an approach enables real-time assessment of state of health (SoH) and supports predictive maintenance, improving reliability and extending the operational lifespan of electronic systems relying on Li-ion batteries.

Future work should focus on developing compact electronic modules for impedance monitoring, exploring their integration with microcontroller-based BMS and communication interfaces, and validating performance under real-world telecommunication and power electronics scenarios.

References

[1] H. Watanabe, S. Omoto, Y. Hoshi, I. Shitanda, and M. Itagaki, "Electrochemical impedance analysis on positive electrode in lithium-ion battery with galvanostatic control," *Journal of Power Sources*, vol. 507, 2021, Art. no. 230258. https://doi.org/10.1016/j.jpowsour.2021.230258

[2] M. Itagaki, K. Honda, Y. Hoshi, and I. Shitanda, "In-situ EIS to determine impedance spectra of lithium-ion rechargeable batteries during charge and discharge cycle," *Journal of Electroanalytical Chemistry*, vol. 737, pp. 78–84, 2015. https://doi.org/10.1016/j.jelechem.2014.06.004

[3] J. Huang, J. Zhang, Z. Li, S. Song, and N. Wu, "Exploring differences between charge and discharge of LiMn2O4/Li half-cell with dynamic electrochemical impedance spectroscopy," *Electrochimica Acta*, vol. 131, pp. 228–235, 2014. https://doi.org/10.1016/j.electacta.2014.02.030

[4] S. Sudaryanto, Y. Purwamargapratala, E. Yulianti, W. Honggowiranto, and E. Kartini, "Electrochemical impedance spectroscopy study of LiFePO4/Li during discharging process," in *IOP Conf. Ser.: Mater. Sci. Eng.*, vol. 924, 2020, Art. no. 012035. https://doi.org/10.1088/1757-899X/924/1/012035

[5] A. Kallel, H. Nouri, T. Keutel, H. Boughanmi, A. Fischer, and O. Kanoun, "Unipolar excitation signal with two phases for impedance spectroscopy of Li-ion battery cells," in *Proc. IEEE Int. Instrum. Meas. Technol. Conf. (I2MTC)*, Kuala Lumpur, Malaysia, May 22–25, 2023, pp. 01–06. https://doi.org/10.1109/I2MTC53148.2023.10176059

[6] A. Barai, G. Chouchelamane, Y. Guo, A. McGordon, and P. Jennings, "A study on the impact of lithium-ion cell relaxation on electrochemical impedance spectroscopy," *Journal of Power Sources*, vol. 280, pp. 74–80. https://doi.org/10.1016/j.jpowsour.2015.01.097

[7] S. Hori and R. Kanno, "Impedance variation of all-solid-state battery cell using Li10GeP2S12; states-of-charges dependence visualized by distribution-of-relaxation time analysis," presented at *243rd ECS Meeting*, Boston, USA, May 28–June 2, 2023. https://doi.org/10.1149/MA2023-022324mtgabs

[8] O. Mendoza-Hernandez, E. Hosono, D. Asakura, H. Matsuda, A. Pfrang, Á. Kriston, M. Umeda, and Y. Sone, "Effect of the charge process on the performance of Li-ion cells during charge-discharge cycling at 0°C," *Electrochemistry*, 2020. https://doi.org/10.5796/electrochemistry.20-00052

[9] M. Oldenburger, B. Bedürftig, A. Gruhle, F. Grimsmann, E. Richter, R. Findeisen, and A. Hintennach, "Investigation of the low frequency Warburg impedance of Li-ion cells by frequency domain measurements," *Journal of Energy Storage*, 2019. https://doi.org/10.1016/j.est.2018.11.029

[10] M. Heinrich, N. Wolff, S. Seitz, and U. Krewer, "Identifying anode and cathode contributions in Li-ion full-cell impedance spectra," *Batteries*, 2022. https://doi.org/10.3390/batteries8050040

[11] B. Zhang, L. Wang, Y. Zhang, X. Wang, Y. Qiao, and S. Sun, "Reliable impedance analysis of Li-ion battery half-cell by standardization on electrochemical impedance spectroscopy (EIS)," *The Journal of Chemical Physics*, vol. 158, 2023, Art. no. 054202. https://doi.org/10.1063/5.0139347

[12] N. Meddings, M. Heinrich, F. Overney, J. Lee, V. Ruiz, E. Napolitano, S. Seitz, G. Hinds, R. Raccichini, M. Gaberšček, and J. Park, "Application of electrochemical impedance spectroscopy to commercial Li-ion cells: A review," *Journal of Power Sources*, 2020. https://doi.org/10.1016/j.jpowsour.2020.228742

[13] S. Zhang, K. Xu, and T. Jow, "Electrochemical impedance study on the low temperature of Li-ion batteries," *Electrochimica Acta*, vol. 49, pp. 1057–1061, 2004. https://doi.org/10.1016/j.electacta.2003.10.016

[14] C. Love and K. Swider-Lyons, "Impedance diagnostic for overcharged lithium-ion batteries," *Electrochemical and Solid State Letters*, vol. 15, 2012. https://doi.org/10.1149/2.014204esl

[15] EEMB, "LIR18650 2600mAh," 2025. [Online]. Available: https://www.eemb.com/product-14 [Accessed: Jun. 29, 2025].

[16] Nexun, "Ogniwo Li-ion EVE ICR18650-26V 2550mAh 7.65A," 2025. [Online]. Available: https://nexun.pl/pl/products/ogniwo-li-ion-eve-icr18650-26v-2550mah-7-65a-1265.html [Accessed: Jun. 29, 2025].

[17] Nexun, "Ogniwo Li-ion Samsung INR18650-35E 3500mAh 8A," 2025. [Online]. Available: https://nexun.pl/pl/products/ogniwo-li-ion-samsung-inr18650-35e-3500mah-8a-1292.html [Accessed: Jun. 29, 2025].

[18] K. Kuliński and A. Nowrot, "A fast method of identifying rechargeable batteries condition and defects," in *MAPE 2018: XV Int. Conf. Multidisciplinary Aspects of Production Engineering*, Zawiercie, Poland, Sep. 5–8, 2018, pp. 301–305. https://doi.org/10.2478/mape-2018-0038